

Pionic fusion of ${}^4\text{He} + {}^{12}\text{C}$ using the ParTI array

A. Zarrella, A. Bonasera, J. Gauthier, L. Heilborn, A. Jedele, A.B. McIntosh,
A. Rodriguez Manso, and S.J. Yennello

Pionic fusion is the process by which two nuclei fuse and then deexcite by the exclusive emission of a pion. The resulting compound nucleus is left in or near its ground state [1]. The process requires that nearly all of the available kinetic and potential energy in the colliding system be concentrated into two degrees of freedom - the rest mass and kinetic energy of the emitted pion. Thus, the energy of the emitted pion is limited by the number of available final states of the fusion residue [2]. The combination of limited available energy and the extreme coherence required in the process ensures that the pionic fusion channel is greatly suppressed. Indeed, the measured pionic fusion cross sections range from hundreds of nanobarns for the lightest systems (He + He) to hundreds of picobarns as one moves to larger systems ($A_{\text{tot}} = 6 - 24$) [2-12].

An experimental effort to measure the pionic fusion process at the Cyclotron Institute was undertaken in August of 2016 when the Momentum Achromat Recoil Spectrometer (MARS) [13] and the Partial Truncated Icosahedron (ParTI) phoswich array [14] were used to perform a coincidence measurement of pionic fusion from the ${}^4\text{He} + {}^{12}\text{C}$ reaction. Pionic fusion events of interest will produce a π^+ which will potentially be detected in the ParTI array and a ${}^{16}\text{N}$ residue which will potentially be detected at the back of MARS. The analysis for that experiment is currently underway. In addition to the pionic fusion experiment, four ParTI phoswich detectors were transported to the Paul Scherrer Institute (PSI) facility in Switzerland where the detector response from incident charged pions was characterized. Using the data from the PSI experiment and the data from the phoswich calibration experiment from 2015, a calibration method was developed for the ParTI array [14].

For the pionic fusion experiment, the K500 Superconducting Cyclotron at the Texas A&M University Cyclotron Institute was used to produce a beam of 55 MeV/u ${}^4\text{He}$ particles which was impinging on a ${}^{12}\text{C}$ target in the MARS beamline. MARS was used to separate reaction products produced around 0° and transport them to the focal plane where they were detected using a silicon stack. The front silicon in the stack was a 5 cm x 5 cm position-sensitive strip detector and the second silicon was a 5 cm x 5 cm single area detector. MARS was tuned to 4 different magnetic rigidities which sampled energy windows inside the kinematically allowed range of pionic fusion residues. Also, background data was taken directly above and below the allowed rigidity range.

During the course of the experiment, it was determined that the position-sensitive silicon detector's thickness varied substantially over the active area. As a result, at the end of the experiment an ${}^{17}\text{O}$ beam was transported to the back of MARS and scanned across the face of the detector in order to map the thickness by measuring the energy loss of the beam as a function of position on the detector. The result of that measurement can be seen in Fig. 1 which shows the 3-dimensional detector thickness map. Using this information, the two silicons in the stack were energy-calibrated. Fig. 2 shows the E_{tot} vs. Y-position particle separation at the back of MARS. Due to the nature of MARS, the Y-position is a measurement of the particle's mass-to-charge ratio. On the detector are spots corresponding to the $A = 2Q$

+ 1 line (where A is the number of nucleons and Q is the charge state of the fragment) and the $A = 2Q + 2$ line. The $A = 2Q + 1$ line begins with $A = 7$, $Q = 3$ at around 17 MeV and ends with $A = 15$, $Q = 7$ at around 45 MeV. The $A = 2Q + 2$ line begins with $A = 12$, $Q = 5$ at around 29 MeV and ends with $A = 18$, $Q = 8$ at around 49 MeV.

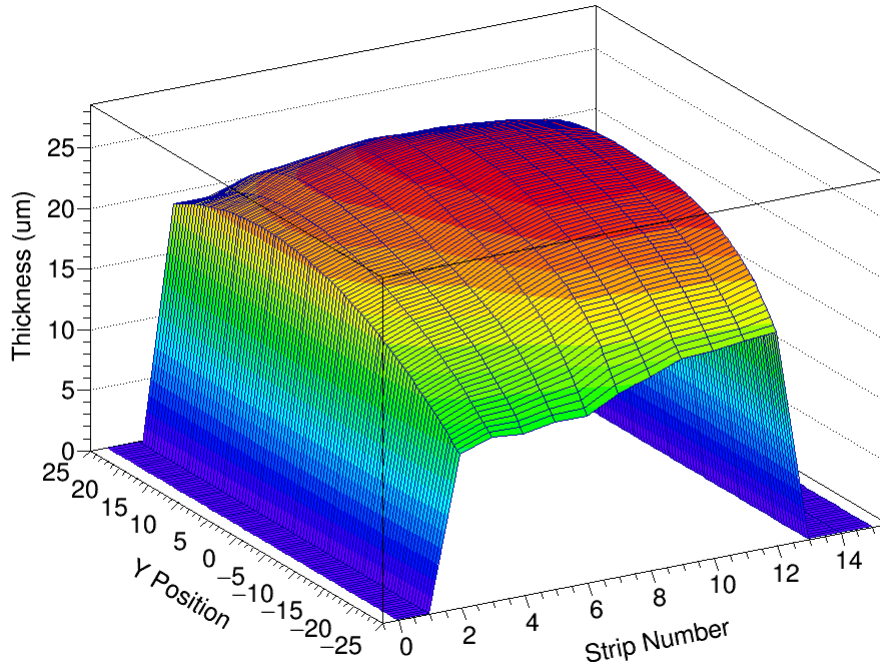


FIG. 1. The measured thickness over the face of the strip silicon detector used in the pionic fusion experiment. On the x-axis is the strip number of the X1 type detector, on the y-axis is the y-position along each strip of the detector. Along the z-axis is the thickness in microns measured at that detector position.

The separation in Fig. 2 is not sufficient, however, to identify specific particle species due to charge state ambiguity. The $^{16}\text{N}^{7+}$ particles of interest, for instance, are indistinguishable from $^{16}\text{O}^{7+}$ in this particle identification space. In order to solve this problem, the dE (energy deposited in the strip silicon) can be plotted as a function of the sampled thickness of the detector from the detector map in Fig. 1 for particles in a single E_{tot} vs. Y -position spot where $E_{\text{tot}} = dE + E$. Fig. 3 is an example of this process for the $A = 12$, $Q = 5$ spot. A clear separation between $^{12}\text{B}^{5+}$ and $^{12}\text{C}^{5+}$ can be seen. The current state of the MARS analysis is concentrated on incorporating the various efficiencies and uncertainties necessary for producing production cross sections for the detected species.

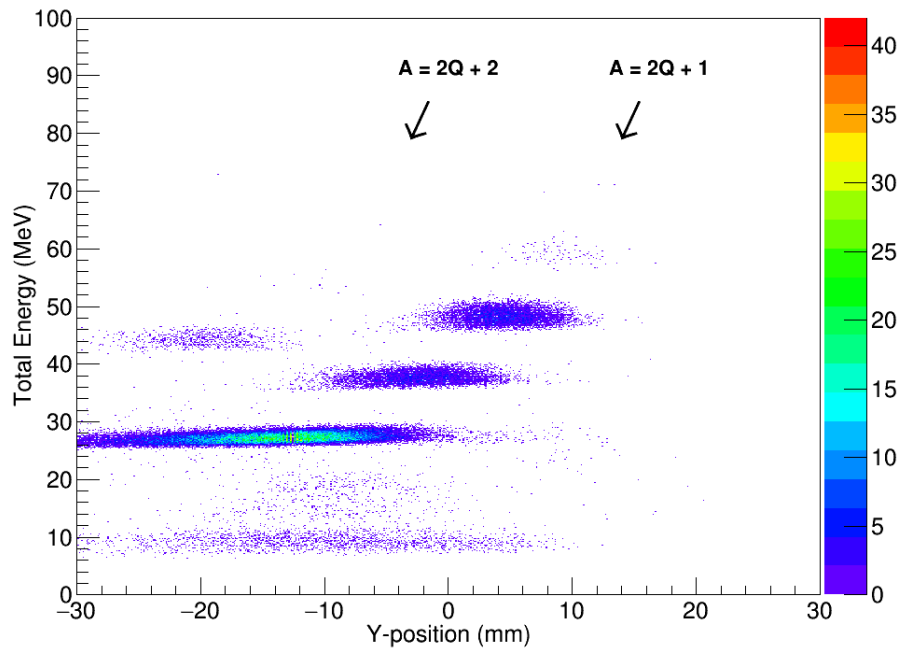


FIG. 2. The total energy vs. y-position plot produced by residues at the back of MARS. The spots correspond to single mass and charge species.

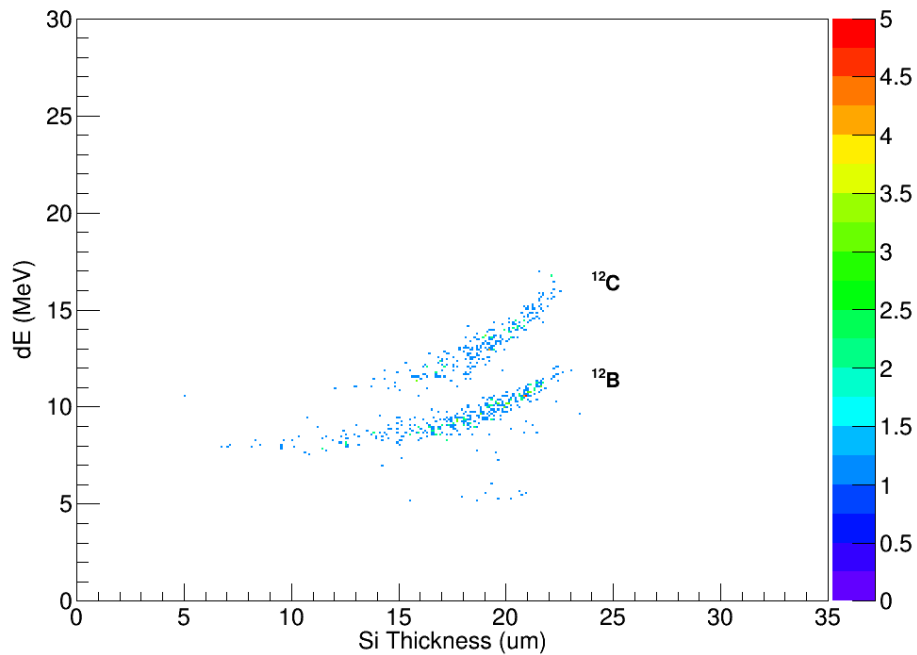


FIG. 3. A plot of the energy deposited in the strip silicon vs. the thickness sampled by the particle for only particles inside the $A = 12$, $Q = 5$ spot from Fig. 2. This plot separates particle species by atomic number.

The second major experimental effort from the last year was the ParTI phoswich characterization experiment which was conducted at PSI. The ParTI array was designed for use in the pionic fusion experiment for the purpose of identifying charged pions. It is comprised of 15 plastic/CsI(Tl) phoswiches arranged on the faces of a truncated icosahedron geometry. The phoswiches were mounted at the back of the π M1 beamline where charged pions were degraded by a variable-thickness copper degrader array and impinged on the ParTI detectors. The detector responses were recorded using the SIS3316 digitizer [15]. These charged pion events are the first examples of charged pion implantations in the ParTI phoswiches. Fig. 4 shows digitized waveforms from the PSI experiment – a π^+ event in panel (a) and a π^- event in panel (b). Both of these waveforms display the characteristic muon decay pulses following the initial implantation pulses which identify them as pion primary events.

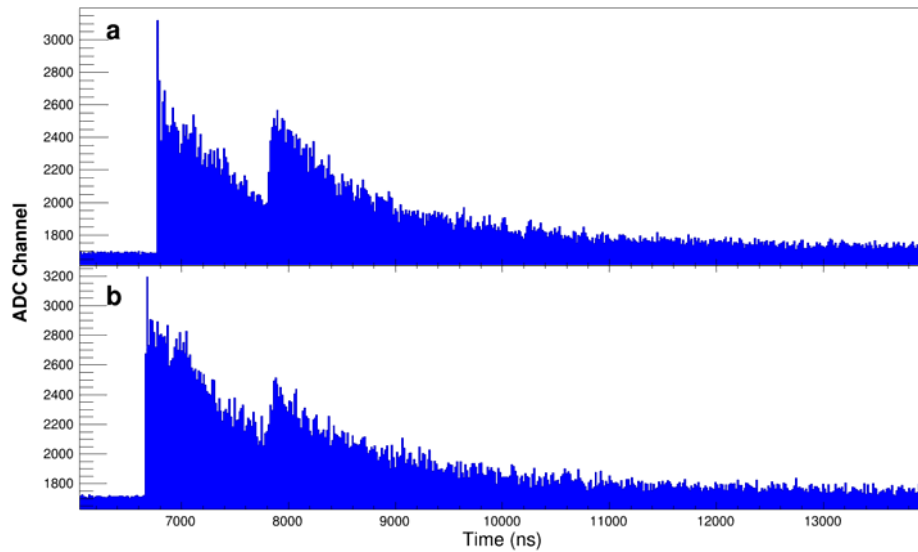


FIG. 4. Examples of phoswich response waveforms with a muon decay secondary pulse for a π^+ (a) and π^- (b) event. On the horizontal axis is time in nanoseconds and the vertical axes are the digitized channel recorded by the SIS3316. The initial response is due to the implantation of the charged particle in the phoswich. The second peak in the response is produced by the decay of the muon implanted in the detector and is a characteristic of a pion primary event.

Independent of the presence of the muon decay peak, a fast vs. slow pulse shape analysis can be performed on the charged particle implantation pulses to produce particle identification lines. Fig. 5 shows these particle identification lines from the PSI experimental runs. On the vertical axis is the integrated fast signal from the phoswich response which is proportional to the energy deposited in the plastic scintillator component of the phoswich. The horizontal axis is the integrated slow signal which is proportional to the energy deposited in the CsI(Tl) component of the phoswich. In both panels, lines can be seen corresponding to pion, proton, and deuteron events (labeled π , p, and d, respectively). In panel (a), the pion line is produced by a π^+ beam and in panel (b) the pion line is produced by a π^- beam. The dearth of events in the π^- line is impacted by the absorption of the pions by nuclei in the detector. The effectiveness of the muon decay trigger system that was developed for the SIS3316 was also explored

during the PSI experiment. It was found that the muon decay trigger increased the ratio of pion events to background events by approximately an order of magnitude.

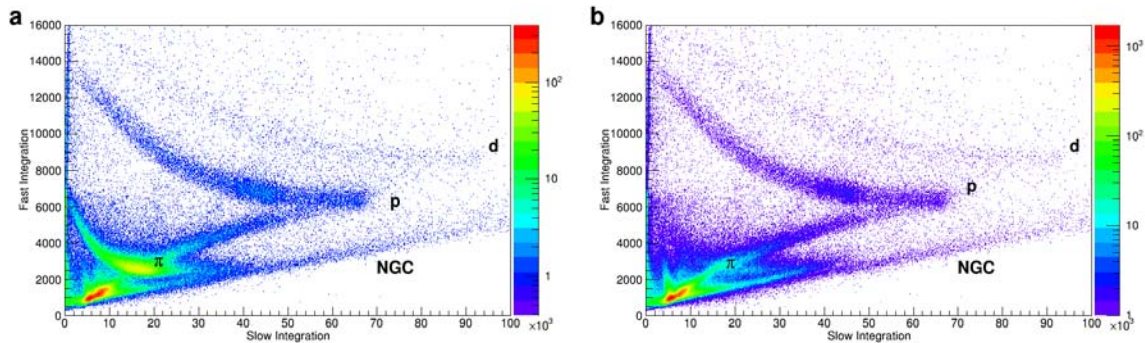


FIG. 5. Data for proton and π^+ beams (a) and proton and π^- beams (b) collected during the PSI experiment. The vertical axes are the fast integrations of the waveforms from the implantation of the charged particles in the phoswich. The horizontal axes are the slow integrations of the waveforms. Moving upward from 0 on the fast integration axis is the neutron/gamma/cosmic (NGC) line, a region corresponding to position (electron) events in panel a (b), a line corresponding to charged pions, the line corresponding to protons, and the line corresponding to deuterons.

Over the course of the next year, the analysis of residues collected at the back of MARS will continue through the inclusion of various detection and instrument efficiencies. This will result in measured cross sections for all species identified. The data collected by the ParTI array during the pionic fusion experiment will be calibrated using the PSI data and the method detailed in reference [14]. The search will then begin for pionic fusion coincidences - a ^{16}N fusion residue at the back of MARS in the same event as a charged pion in the ParTI array.

- [1] P. Braun-Munzinger and J. Stachel. *Ann. Rev. Nucl. Part. Sci.* **37**, 97 (1987).
- [2] D. Horn, *et al.* *Phys. Rev. Lett.* **77**, 2408 (1996).
- [3] Y. Le Bornec, *et al.* *Phys. Rev. Lett.* **47**, 1870 (1981).
- [4] L. Joulaeizadeh, *et al.* *Phys. Lett. B* **694**, 310 (2011).
- [5] W. Schott, *et al.* *Phys. Rev. C* **34**, 1406 (1986).
- [6] M. Andersson, *et al.* *Nucl. Phys.* **A779**, 47 (2006).
- [7] M. Andersson, *et al.* *Phys. Lett. B* **481**, 165 (2000).
- [8] M. Andersson, *etal.* *Phys. Scr.* **T104**, 96 (2003).
- [9] L. Bimbot, *et al.* *Phys. Rev. C* **30**, 739 (1984).
- [10] L. Bimbot, *et al.* *Phys. Lett. B* **114**, 311 (1982).
- [11] J. Homolka, *et al.* *Phys. Rev. C* **38**, 2686 (1988).
- [12] N. Willis, *et al.* *Phys. Lett. B* **136**, 334 (1984).
- [13] R.E. Tribble, *et al.* *Nucl. Instrum. Methods Phys. Res.* **A285**, 441 (1989).
- [14] A. Zarrella, *et al.* *Physics Procedia* (Accepted).
- [15] <http://www.struck.de/sis3316.html>.